

## Macroscopic effects of the perturbation of the particle velocity distribution in a trigger wave

A. Lemarchand<sup>1,\*</sup> and B. Nowakowski<sup>2,†</sup>

<sup>1</sup>*Laboratoire de Physique Théorique des Liquides, Université Pierre et Marie Curie, CNRS UMR 7600, 4, Place Jussieu, 75252 Paris Cedex 05, France*

<sup>2</sup>*Institute of Physical Chemistry, Polish Academy of Sciences, Kasprzaka 44/52, 01-224 Warsaw, Poland*

(Received 22 November 1999)

Departure from the equilibrium particle velocity distribution induced by a chemical reaction is studied in an inhomogeneous chemical bistable system in which a trigger wave can propagate. These nonequilibrium effects influence the speed and shape of the trigger wave propagating between the two stable stationary states. In contrast to the Fisher front, the discretization of the variables and the internal fluctuations do not sensitively modify the macroscopic properties of the trigger wave. Analytical results deduced from the Boltzmann equation agree well with microscopic simulations using Bird's method. Both approaches lead to large relative corrections to the front speed, in particular for parameter values close to that corresponding to a stationary interface between the two stable states.

PACS number(s): 05.70.Ln, 51.10.+y, 82.20.Wt, 82.20.Mj

### I. INTRODUCTION

Kinetic theory studies based on the Boltzmann equation have revealed that the perturbation of the particle velocity distribution induced by a chemical reaction may significantly influence the dynamics of gaseous chemical systems [1–4]. The departure from the equilibrium distribution comes from the dependence of molecule reactivity on energy, so that a chemical process affects more strongly the populations of reactant molecules in a certain range of velocities. The consequence of this nonequilibrium effect at a macroscopic level is a modification of the rate constants and transport coefficients appearing in the macroscopic equations for the concentrations of chemical species.

In this paper, we study the perturbation of the particle velocity distribution induced by a reaction in a bistable inhomogeneous chemical system. Our objective is to study the influence of such a nonequilibrium effect on the macroscopic properties of a wave front propagating between the two stable stationary states of the system. We examine a chemical model with a third order reaction that was originally introduced by Schlögl [5] to compare a bifurcation in an open system with the liquid-gas phase transition. Depending on the values of the rate constants, the reaction-diffusion equation associated with the Schlögl model admits either one or three homogeneous stationary states. In this last case and for adequately chosen initial and boundary conditions, it possesses a unique wave-front solution, called the trigger wave, connecting the two stable stationary states [6]. The propagation speed and the profile width of the front depend on the rate constants and on the diffusion coefficient of the chemical species. Consequently, the corrections to the rate coefficients due to perturbations of the particle velocity distribution may modify the values of the macroscopic properties of the front. Moreover, a previous study [7] of the Schlögl model in homogeneous conditions has revealed that the per-

turbation of local equilibrium shifts the values of the stationary states, especially in the vicinity of a bifurcation. It can therefore be expected that the level of the plateau in the trigger front will be modified in the presence of a perturbation of the particle velocity distribution. The original Schlögl model involves reservoirs of chemical species. Keeping constant the concentrations of these species maintains the system out of chemical equilibrium. To avoid the costly simulation [7,8] of such reservoirs in the numerical procedure, in this paper we consider the following modified Schlögl model:



This reaction scheme differs somewhat from Schlögl's original one, used in our previous study of homogeneous systems [7], but it also leads to third order reaction kinetics and bistability. The second reaction is supposed to be irreversible, so that one of the stable stationary states is associated with a vanishing concentration of species A. Since reactions (1) and (2) do not proceed without A particles, there are no chemical fluctuations within the domain occupied by this state. Thus, if this is the receding stable state of the front, then we avoid nucleation phenomena that could switch the system locally to another stable state and create other spots of origin of front propagation. We assume that reaction (2) is induced by an interaction with the exterior; for example, it may be a photochemical reaction. For this reason, the system is open, out of chemical equilibrium, and may exhibit multiple stable stationary states.

The number of molecules is conserved by the above reactions and it can be assumed that the total concentration of both species  $n = n_A + n_B$  is homogeneous and stationary. Under this constraint, only one of the equations governing the macroscopic dynamics of the concentrations is independent. Moreover, if the initial condition depends only on one (let us say  $x$ ) coordinate, the inhomogeneity will be of this form all

\*Email address: anle@lptl.jussieu.fr

†Email address: bogm@ichf.edu.pl

the time. The standard reaction-diffusion equation for the concentration  $n_A$  of species  $A$  can then be written as

$$\frac{\partial n_A}{\partial t} = -(k_1^{(0)} + k_{-1}^{(0)})n_A^3 + k_1^{(0)}n_A^2n - k_2n_A + D \frac{\partial^2 n_A}{\partial x^2}, \quad (3)$$

where  $D$  is the diffusion coefficient, and  $k_i^{(0)}$  are reaction rate constants unperturbed by the nonequilibrium effects. In order to investigate the effect of nonequilibrium velocity distributions in the modified Schlögl model with reactions (1) and (2), we consider the Boltzmann equation for the distribution functions  $f_\alpha(x, \mathbf{v}, t)$  for position  $x$  and velocity  $\mathbf{v}$  of species  $\alpha = A, B$ . To simplify computations, we choose a model of reactive hard spheres already used in previous works involving microscopic simulations of chemical systems [9–11]. The molecules are considered as hard spheres with identical mass  $m$  and diameter  $d$ , which differ only by their chemical identity. These chemical properties are changed in reactive collisions occurring when collision partners correspond to a given reaction and if a condition following from a molecular reaction cross section is satisfied. The essential property we assume is that no heat is released in the reaction: Then, apart from the chemical effect, the particle velocities are transformed in a reactive collision as in an elastic one. More specifically, we set up the reaction cross section by cutting out a part of the original cross section of nonreactive hard spheres. Thus, for an observer blind to the chemical aspect, all collisions are elastic, and the system seems as if it consists of simple hard spheres. Consequently, if we assume that the mixture as a whole is initially in mechanical equilibrium, it remains in this state all the time. Accordingly, the distribution function for the whole mixture satisfies the condition

$$\begin{aligned} F(v) &= f_A(x, \mathbf{v}, t) + f_B(x, \mathbf{v}, t) \\ &= n(m/2\pi kT)^{3/2} \exp(-mv^2/2kT) \\ &\equiv n\psi_0(v), \end{aligned} \quad (4)$$

where  $\psi_0(v)$  is the normalized equilibrium Maxwellian distribution function for velocities of molecules of mass  $m$  in a system at temperature  $T$ . Condition (4) can also be derived rigorously from the kinetic equations consistent with the properties introduced above. However, the velocity distributions of individual components in nonequilibrium conditions are not Maxwellian, and the concentrations of the species

$$\int f_\alpha(x, \mathbf{v}, t) d\mathbf{v} = n_\alpha(x, t), \quad \alpha = A, B, \quad (5)$$

depend on position  $x$  and time  $t$ . When reactive collisions are less frequent than elastic collisions, the velocity distributions of reactive species can be obtained from a perturbative solution of the Boltzmann equations [1,3].

We verify analytical calculations of nonequilibrium effects by comparing them with microscopic simulations. In contrast to actual experiments, microscopic simulations may be performed using exactly the same assumptions as in the theoretical approach. The direct simulation Monte Carlo (DSMC) method, initially proposed by Bird [12], introduces a stochastic treatment of binary collisions that relies on the same hypotheses as the Boltzmann equation and speeds up

the simulation time by two or three orders of magnitude with respect to actual molecular dynamics. The Bird method has already been successfully used to simulate reactive systems [9–11] and may be directly compared with the theoretical predictions.

The results of the macroscopic deterministic description of a trigger wave based on reaction scheme (1) and (2) are briefly recalled in the next section. In Sec. III we present the Boltzmann equation associated with the Schlögl model and obtain the solution of this equation by means of a perturbative method [1,3]. The corrections to the macroscopic reaction-diffusion equation (3) for the concentration of species  $A$  are calculated using this solution. The procedure followed to perform the microscopic simulations is given in Sec. IV and the analytical predictions are compared with the simulation results in Sec. V. Section VI contains conclusions.

## II. MACROSCOPIC DESCRIPTION OF A TRIGGER WAVE

In the bistability domain, the macroscopic equation (3) admits three stationary states obeying

$$A_{1,2}^{(0)} = \frac{k_1^{(0)}n}{2(k_1^{(0)} + k_{-1}^{(0)})} (1 \pm b), \quad (6)$$

$$A_3^{(0)} = 0, \quad (7)$$

with

$$b^2 = 1 - 4(k_1^{(0)} + k_{-1}^{(0)})k_2/(k_1^{(0)}n)^2 \geq 0. \quad (8)$$

We choose  $b = (A_1^{(0)} - A_2^{(0)})/(A_1^{(0)} + A_2^{(0)})$  as the control parameter to measure the distance from the two bifurcations associated with the values  $b=0$  and  $b=1$ . In the bistability region, the parameter  $b$  obeys  $0 \leq b \leq 1$ . The critical value  $b=0$  ( $b=1$ ) corresponds to the coalescence of the unstable stationary state  $A_2^{(0)}$  with the stable one  $A_1^{(0)}$  ( $A_3^{(0)}$ ). Equation (3) admits a single wave front propagating at a constant speed  $U$  and connecting the two stable stationary states  $n_A = A_1^{(0)}$  and  $n_A = 0$ :

$$n_A(\zeta) = A_1^{(0)} \frac{\exp(-4\zeta/E)}{1 + \exp(-4\zeta/E)}, \quad (9)$$

where  $\zeta = x - Ut$  is a coordinate in the frame moving with the front, and  $E$  is the profile width deduced from the steepness at the inflection point,

$$E = \frac{4\sqrt{2}}{A_1^{(0)}} \left( \frac{D}{k_1^{(0)} + k_{-1}^{(0)}} \right)^{1/2}. \quad (10)$$

The speed  $U$  of the front propagation,

$$U = \left( \frac{(k_1^{(0)} + k_{-1}^{(0)})D}{2} \right)^{1/2} (A_1^{(0)} - 2A_2^{(0)}), \quad (11)$$

is uniquely prescribed by the dynamics; it depends only on the rate coefficients in the reaction-diffusion equation. In the following, we impose the condition

$$A_2^{(0)} < \frac{A_1^{(0)}}{2} \quad (12)$$

so that the propagation speed remains positive. From the above condition it follows that

$$1/3 < b \leq 1. \quad (13)$$

We explain below that the propagation of the front in the opposite direction would present a problem in the microscopic simulation procedure in the presence of a perturbation of local equilibrium. Note, however, that condition (13) prevents one from studying the vicinity of the bifurcation associated with  $b=0$ , i.e., with the coalescence of  $A_2^{(0)}$  and  $A_1^{(0)}$ . We know from a former analysis of the Schlögl model in homogeneous conditions [7] that it is precisely in the vicinity of this bifurcation that even small nonequilibrium effects are sensitively amplified by the dynamical system, leading to very large macroscopic effects, like a diverging correction to the nonvanishing stable stationary state. Nevertheless, the trigger wave, with its uniquely defined speed, appears as a good candidate for the analysis of the nonequilibrium effects induced by a reaction, because other possible sources of disturbance do not lead to significant effects in this system. This is not true for a wave front propagating into an unstable state as in the Fisher model [13]. In this case, the existence of a continuous family of propagation speeds associated with stable front solutions [14] makes the system sensitive to several perturbations of different nature. In particular, the discretization of the variables occurring when switching from concentrations to particle numbers [15,16] and the internal fluctuations [16,17] present in microscopic simulations are known to modify the speed of this kind of wave front. All these effects of different origin interfere and it is therefore difficult to isolate the nonequilibrium effects in microscopic simulations of the Fisher front [11,16]. Stochastic descriptions of the trigger wave at a mesoscopic level prove that the effects of internal fluctuations [18] and variable discretization [19] arise only in very small systems and decrease as  $\Omega^{-3/2}$ , where  $\Omega$  characterizes the system size. For the system studied in this paper, these effects can be neglected.

### III. BOLTZMANN EQUATION FOR THE SCHLÖGL MODEL

Our treatment of the Boltzmann equation follows a previous work [20] which presented the solution of the kinetic equation for an inhomogeneous binary mixture with bimolecular reactions. However, a specific problem arises in the Schlögl model in relation to the existence of ternary collisions according to reaction (1). Introduction of processes with simultaneous interactions of three or more molecules poses a particular problem in the model of hard spheres. To mimic this kind of collision we use the solution already adopted in microscopic simulations of the Brusselator model [10]. In the case of the forward reaction (1), we first determine the reaction cross section for binary collision ( $A$ - $B$ ). When this kind of encounter occurs, it is regarded as a ternary collision ( $A$ - $B$ )- $A$  if an  $A$  molecule is in the nearest neighborhood of the colliding pair ( $A$ - $B$ ). It can be assumed that in such a small volume concentrations are uniform, and

consequently the probability of finding an  $A$  particle around position  $\mathbf{r}$  of the colliding ( $A$ - $B$ ) pair is equal to the concentration fraction  $n_A(\mathbf{r})/n$ , or, in terms of the velocity distribution, it is  $\int f_A d\mathbf{v}/n$ . The exclusion correction is omitted, as usual in the Boltzmann treatment. Thus, the term for the termolecular ( $A$ - $B$ )- $A$  reactive collisions consists of the usual factor for binary ( $A$ - $B$ ) reactive collisions multiplied by the probability factor given above. For reasons that will be explained further, only this combination is accepted for the forward reaction (1), while the combination of ( $A$ - $A$ ) and  $B$  as a third partner is excluded. Triple collisions ( $A$ - $A$ )- $A$  are handled in the same fashion. The procedure used to introduce three-molecular reactions can be explained in terms of the two-step mechanism: A binary collision is regarded as the formation of a molecular complex with a certain lifetime and the subsequent weak interaction of this doublet with a third, nearest molecule yields effectively a termolecular process [21]. The second stage can be treated as an induction effect, which is much faster than the first one, and the rate of such a termolecular reaction is determined effectively by the frequency of the relevant binary collisions. Equivalently, in the framework of the quasistationary state approximation [22], the termolecular process is usually obtained by elimination of a very reactive intermediate step. This approach corresponds to the formulation of ternary collisions in standard chemical kinetics [23]. In the rigorous approach in kinetic theory, many-particle collision terms involve sequences of binary encounters of hard spheres with velocities correlated due to recollisions or cyclic collisions [24]. Our implementation of ternary collisions relies on a simpler decomposition, in which a bimolecular stage is described by the usual Boltzmann term for binary collisions.

As a molecular reaction model, we apply in this paper the line-of-centers model that has been extensively used in previous theoretical work [3,4,20] and simulations [4,9,11,25]. In a reactive encounter, the relative velocity  $\mathbf{g}$  of molecules in a direct binary collision must satisfy the condition

$$\mathbf{e} \cdot \mathbf{g} \geq g^*, \quad (14)$$

where  $\mathbf{e}$  denotes the unit vector along the line connecting the centers of the hard spheres at the instant of impact, and  $g^*$  is the threshold relative velocity. From condition (14) it follows that the energy of the relative motion in a reactive collision exceeds the value (in units of  $kT$ )

$$\epsilon = \frac{m g^{*2}}{4kT}. \quad (15)$$

Thus,  $\epsilon$  is the activation energy of the reaction. Moreover, the reaction is effective with the probability given by the steric factors  $s_{\pm 1}$  associated with forward and reverse reactions (1). There is no reaction heat, and thus the detailed balance condition requires that for reaction (1) the cross sections for the forward ( $\sigma_1^*$ ) and reverse ( $\sigma_{-1}^*$ ) processes are proportional [20],

$$\frac{\sigma_1^*}{s_1} = \frac{\sigma_{-1}^*}{s_{-1}} = \sigma^*. \quad (16)$$

The steric factors  $s_1$  and  $s_{-1}$  give the conditional probability that molecules actually react, provided the energetic condition imposed by the cross section  $\sigma^*$  is satisfied. Let us recall that, in the molecular model of reactive hard spheres, the cross sections for elastic collisions ( $\sigma^e$ ) and reactive collisions ( $\sigma^*$ ) of molecules of the same species sum up to the cross section of nonreactive particles. For example, for  $A$ - $B$  collisions [which are also involved in the bimolecular step of forward reaction (1)] this means that  $\sigma_{AB}^e + (n_A/n)\sigma_1^* = \sigma_0$ .

Taking into account the assumptions introduced above, it can easily be checked that the Boltzmann equation for the total distribution function  $F = f_A + f_B$  is a closed equation that does not contain terms for reactive collisions. The spatially uniform Maxwellian distribution is then a stable stationary solution for  $F$ —this formally justifies condition (4) for the distribution functions of the species. Due to this condition, it is sufficient to consider a kinetic equation for only one species in the Schlögl model; for component  $A$  the Boltzmann equation has the form

$$\begin{aligned} \frac{\partial f_A}{\partial t} + \mathbf{v} \cdot \frac{\partial f_A}{\partial \mathbf{r}} = & J(f_A) + s_1 \left( \int f_B(\mathbf{v}') f_A(\mathbf{v}_1') g d\sigma^* d\mathbf{v}_1 \right) \\ & \times \frac{\int f_A(\mathbf{v}) d\mathbf{v}}{n} - s_{-1} \\ & \times \left( \frac{1}{2} \int f_A(\mathbf{v}') f_A(\mathbf{v}_1') g d\sigma^* d\mathbf{v}_1 \right) \\ & \times \frac{\int f_A(\mathbf{v}) d\mathbf{v}}{n} - k_2 f_A. \end{aligned} \quad (17)$$

Only velocities are indicated explicitly as arguments of  $f_\alpha$  in the collision integrals, the primes denote postcollisional velocities, and  $g = |\mathbf{v} - \mathbf{v}_1|$ . The term  $J(f_A)$  includes all integrals for elastic collisions. As shown in previous papers [7,20], due to constraint (4) for the distribution functions, it can be transformed into the following simple form:

$$J(f_A) = \int [f_A(\mathbf{v}') F(v_1') - f_A(\mathbf{v}) F(v_1)] g d\sigma_0 d\mathbf{v}_1. \quad (18)$$

It is worth noting that  $J(f_A)$  is a *linear* integral operator for  $f_A$ . Moreover,  $J(f_A)$  is self-adjoint, with the scalar product defined as

$$\langle g|f \rangle = \int g(\mathbf{v}) f(\mathbf{v}) [\psi_0(v)]^{-1} d\mathbf{v}. \quad (19)$$

The next two terms on the right side of Eq. (17) describe termolecular reactive collisions related to reactions (1) (according to the approach described above) and the last term represents irreversible reaction (2). Using relation (16), the differential cross sections for reaction (1) are put in the form  $d\sigma_\rho^* = s_\rho d\sigma^*$ ,  $\rho = \pm 1$ , where  $d\sigma^*$  is the differential cross section with condition (14) for energy only.

Equation (17) is solved by means of the Chapman-Enskog perturbative method [26], originally successfully developed for calculation of coefficients for transport processes. This

solution method has been adopted to nonequilibrium chemical kinetics in homogeneous conditions in many previous kinetic theory studies of reactions in gases [1–3]. In the recently presented extension of this approach to inhomogeneous chemical systems [20], the perturbation treatment of simultaneous chemical reactions and diffusion is applied in order to obtain higher order cross effects. The Chapman-Enskog method is valid if transport processes are slow in comparison with the relaxation of the velocity distribution by elastic collisions [26,27]; the same limitation applies also to reactive processes [28,29]. Under this condition, the time and spatial derivatives as well as the collision integrals for reactions can be treated as perturbations of the leading terms related to elastic collisions, which is the collision integral  $J(f_A)$  in the case of Eq. (17). The solution obtained by this method results in a macroscopic reaction-diffusion equation which includes corrections due to the perturbation of the Maxwellian molecular velocity distributions. We adopt here the derivation developed for a two-component chemical mixture with reactions involving binary collisions [20]. The modifications specific to the Schlögl model are related only to the treatment of ternary collisions in reaction (1). We outline below the essential steps of the calculations, and refer to the earlier work [20] for details. The distribution function is expanded in perturbation series as

$$f_A = f_A^{(0)} + f_A^{(1)} + f_A^{(2)} + \dots \quad (20)$$

The introduction of Eq. (20) into the Boltzmann equation (17) yields the expansion of the kinetic equation. The lowest order equation contains the elastic collision integral solely,  $J(f_A^{(0)}) = 0$ . The only solution of this equation is the local equilibrium distribution

$$f_A^{(0)}(\mathbf{r}, \mathbf{v}, t) = n_A \psi_0(v), \quad (21)$$

where  $n_A$  is the number density of molecules  $A$ , and the function  $\psi_0$  is the Maxwellian velocity distribution at temperature  $T$  as for the whole mixture. The lowest order approximation for the dynamics of  $n_A$  is obtained by inserting function (21) into the Boltzmann equation (17) and integrating over velocities. This yields the standard equation for chemical kinetics as if in a homogeneous system,

$$\left( \frac{\partial n_A}{\partial t} \right)^{(0)} = k_1^{(0)} n_A^2 n - (k_1^{(0)} + k_{-1}^{(0)}) n_A^3 - k_2 n_A. \quad (22)$$

The lowest order approximations for rate constants  $k_1^{(0)}$  and  $k_{-1}^{(0)}$  of reaction (1) have the following form for the model of reactive hard spheres considered here:

$$k_1^{(0)} = s_1 \exp(-\epsilon) \frac{4\sigma_0}{n} \left( \frac{kT}{\pi m} \right)^{1/2}, \quad (23)$$

$$k_{-1}^{(0)} = \frac{1}{2} s_{-1} \exp(-\epsilon) \frac{4\sigma_0}{n} \left( \frac{kT}{\pi m} \right)^{1/2}. \quad (24)$$

In this approximation, the Boltzmann equation only justifies the phenomenological law for chemical kinetics. Corrections to the standard rate equation (22) are provided by the next order solution. The Boltzmann equation for higher order terms in expansion (20) involves the time derivative. The

approximation for the so-called normal solutions assumes that the distribution function depends on time only implicitly through the hydrodynamic variables—in this case the concentration  $n_A$  and its gradients. Consequently, the time derivative of the distribution function is calculated as follows:

$$\frac{\partial f_A^{(i)}}{\partial t} = \sum_{k=0}^i \frac{\partial f_A^{(i-k)}}{\partial n_A} \left( \frac{\partial n_A}{\partial t} \right)^{(k)} + \sum_{k=0}^i \frac{\partial f_A^{(i-k)}}{\partial \nabla n_A} \cdot \nabla \left( \frac{\partial n_A}{\partial t} \right)^{(k)} + \dots \quad (25)$$

The time derivatives  $(\partial n_A / \partial t)^{(k)}$  are calculated by integrating over velocities the  $k$ th term of the expansion of the Boltzmann equation, obtained with the use of expansion (20) of the distribution function. Thus, they provide the  $k$ th order approximations to the dynamics of  $n_A$ . Equation (25) eliminates the explicit time derivative from the Boltzmann equation for the higher order terms of the distribution function given in Eq. (20). In this approach, the equation for the first perturbative correction  $f_A^{(1)}$  has the form

$$\nabla n_A \cdot \mathbf{v} \psi_0 - \frac{n_A}{n} \frac{\left( -\frac{1}{2} s_{-1} n_A^2 + s_1 n_A n_B \right)}{n} \times [R(\psi_0) - \langle \psi_0 | R(\psi_0) \rangle \psi_0] = J(f_A^{(1)}). \quad (26)$$

The linear integral operator  $R$  introduced above is

$$R(\phi) = \int \phi(\mathbf{v}') F(v'_1) g d\sigma^* d\mathbf{v}_1. \quad (27)$$

It is related to the integrals for reactive collisions for reaction (1). In the following it is convenient to use the notation

$$Q = \frac{-\frac{1}{2} s_{-1} n_A^2 + s_1 n_A n_B}{n}. \quad (28)$$

We also define the operation

$$\bar{\phi} = \phi - \langle \psi_0 | \phi \rangle \psi_0, \quad (29)$$

where  $\bar{\phi}$  is deduced from  $\phi$  by subtracting its projection onto  $\psi_0$ . Thus,  $\bar{\phi}$  is orthogonal to the kernel of  $J$ , which is spanned only by  $\psi_0$  [the only solution of  $J(f) = 0$ ]. The solution of Eq. (26) can then be written in the form

$$f_A^{(1)} = \frac{n_A}{n} Q \omega(v) + \nabla n_A \cdot \mathbf{v} \chi(v), \quad (30)$$

where functions  $\omega$  and  $\chi$  are the solutions of the following linear integral equations

$$-R(\psi_0) = J(\omega), \quad (31)$$

$$\mathbf{v} \psi_0 = J(\mathbf{v} \chi). \quad (32)$$

The left hand sides of these equations are orthogonal to the kernel of  $J$ , so Eqs. (31) and (32) are well defined. The function  $\omega$  describes the perturbation of the equilibrium velocity distribution caused by the chemical reaction, and  $\mathbf{v} \chi$  provides the anisotropic component of the velocity distribu-

tion related to diffusion. Introducing the first correction  $f^{(1)}$  into the Boltzmann equation and integrating over velocities yields

$$\left( \frac{\partial n_A}{\partial t} \right)^{(1)} = \left( \frac{n_A}{n} \right)^2 Q \frac{dQ}{dn_A} \langle \psi_0 | R(\omega) \rangle + D_0 \Delta n_A. \quad (33)$$

The first term of this equation gives the first order correction to the standard reaction kinetics given in Eq. (3). Note that only multimolecular reactions (1) are effective in perturbing the velocity distribution function  $f_A$ . In particular, the correction to the reaction rate vanishes when reaction (1) is balanced, i.e., for  $Q = 0$ . More specifically, the condition for reaction imposed on the bimolecular step in the model chosen for reactive collisions (1) favors molecules with higher energy. Consequently, reaction results in an energy transfer from reactants to products, but only for the species that participate in a binary collision step. However, the forward reaction (1), which would involve two  $A$  molecules in the binary collision, would not produce a systematic energy flux from one species to the other, since the chemical identity of the partners of this binary complex is not changed in such a realization of the termolecular reaction. For this reason, a combination of a doublet ( $A-A$ ) and  $B$  as a third molecule is not considered as a ternary collision for the forward reaction (1). The unimolecular reaction (2) as a process of internal transformation is independent of collisions, and does not cause any perturbation of the velocity distribution because it involves a uniform sampling from a given  $f_A$ .

The second term of Eq. (33) describes diffusion with a coefficient given by the formula

$$D_0 = -\frac{1}{3} \langle \psi_0 | v^2 \chi \rangle. \quad (34)$$

This result does not involve the chemical process, so that this approximation level gives the same diffusion coefficient as in the nonreactive system [26]. In order to calculate in turn the correction to the transport process, it is necessary to resort to the second order approximation. This involves the reactive collision integrals linearized around  $f^{(0)}$ ,

$$R_+(\phi) = \frac{n_A}{n} \frac{dQ}{dn_A} R(\phi) + \frac{Q}{n} R_-(\phi) - k_2 \phi, \quad (35)$$

where the operator  $R_-$  is given by

$$R_-(\phi) = \int (\phi'_1 F' - \phi' F'_1) g d\sigma^* d\mathbf{v}_1. \quad (36)$$

The equation for  $f^{(2)}$  has the form

$$\begin{aligned} & \left( \frac{d}{dn_A} \frac{n_A}{n} Q \langle \psi_0 | R(\psi_0) \rangle - k_2 \right) \left( \frac{n_A}{n} Q \omega + \nabla n_A \cdot \mathbf{v} \chi \right) \\ & - k_2 \frac{n_A^2}{n} \frac{dQ}{dn_A} \omega + \mathbf{v} \cdot \nabla \frac{n_A}{n} Q \omega + \overline{(\mathbf{v} \cdot \nabla)(\mathbf{v} \cdot \nabla n_A) \chi} \\ & - R_+ \left( \frac{n_A}{n} Q \omega + \nabla n_A \cdot \mathbf{v} \chi \right) = J(f_A^{(2)}). \end{aligned} \quad (37)$$

The solution of this equation is obtained formally by the action of  $J^{-1}$  on both sides of Eq. (37). We consider only the terms of  $f^{(2)}$  containing  $\nabla n_A$ , which contribute to diffusion. They yield the following correction to the diffusion term in the standard macroscopic equation (3):

$$\begin{aligned} \left(\frac{\partial n_A}{\partial t}\right)_{diff}^{(2)} &= \nabla \cdot (D' \nabla n_A) \\ &= -\frac{1}{3} \nabla \cdot \left( \frac{n_A}{n} \frac{dQ}{dn_A} [\langle \psi_0 | R(\psi_0) \rangle \langle \chi | v^2 \chi \rangle \right. \\ &\quad + 2 \langle \omega | v^2 \chi \rangle - \langle \mathbf{v} \chi | R(\mathbf{v} \chi) \rangle] \\ &\quad + \frac{Q}{n} [\langle \psi_0 | R(\psi_0) \rangle \langle \chi | v^2 \chi \rangle \\ &\quad \left. + \langle \omega | v^2 \chi \rangle - \langle \mathbf{v} \chi | R_-(\mathbf{v} \chi) \rangle] \right) \nabla n_A. \end{aligned} \quad (38)$$

Moreover, the Boltzmann equation yields an additional component in the second order dynamic equation for concentration  $n_A$ . This term is related to the nonlinearity of the reactive collision integrals and contains the square of the concentration gradient [20]. For the Schlögl model it has the form

$$\begin{aligned} \left(\frac{\partial n_A}{\partial t}\right)_{nonl}^{(2)} &= \frac{1}{3} (\nabla n_A)^2 \left[ \frac{d}{dn_A} \left( \frac{n_A}{n} \frac{dQ}{dn_A} \right) \langle \omega | v^2 \chi \rangle \right. \\ &\quad \left. + \frac{1}{2} n_A \frac{d^2 Q}{dn_A^2} \int \chi \chi_1 (\mathbf{v} \cdot \mathbf{v}_1) g d\sigma^* d\mathbf{v} d\mathbf{v}_1 \right]. \end{aligned} \quad (39)$$

In order to obtain the explicit form of the corrections to the dynamic equation for  $n_A$ , the solutions  $\omega$  and  $\chi$  of Eqs. (31) and (32) are needed. As usual, these functions are assumed to be in the form of an expansion in Sonine polynomials [26]; its convergence has been examined for both transport [26,27] and chemical processes [3,29]. Two-term solutions are commonly accepted as satisfactory approximations, and allow for use of convenient analytical expressions as well:

$$\omega(v) = \psi_0(v) [a_1 S_{1/2}^{(1)}(c^2) + a_2 S_{1/2}^{(2)}(c^2)], \quad (40)$$

$$\chi(v) = \psi_0(v) [b_0 S_{3/2}^{(0)}(c^2) + b_1 S_{3/2}^{(1)}(c^2)], \quad (41)$$

where  $c^2 = mv^2/2kT$ . The coefficients  $a_i, b_i$  for the model of reactive hard spheres are given by [20]

$$a_1 = -\frac{1}{2} \exp(-\epsilon) \left[ \frac{1}{2} + \epsilon + \frac{1}{30} \left( \frac{3}{4} + 2\epsilon - \epsilon^2 \right) \right], \quad (42)$$

$$a_2 = -\frac{1}{15} \exp(-\epsilon) \left( \frac{3}{4} + 2\epsilon - \epsilon^2 \right), \quad (43)$$

and [26]

$$b_0 = -\frac{59}{58} \frac{3}{32n\sigma_0} \sqrt{\frac{m}{\pi kT}}, \quad b_1 = \frac{4}{59} b_0. \quad (44)$$

The terms (33), (38), and (39) can then be explicitly calculated by quadratures with the above functions  $\omega$  and  $\chi$ . The

modified reaction-diffusion equation including up to second order corrections can be presented in the following form [when restricted like Eq. (3) to one dimension related to the direction  $x$  of the front propagation]:

$$\begin{aligned} \frac{dn_A}{dt} &= [-(k_1^{(0)} + k_{-1}^{(0)})n_A^3 + k_1^{(0)}n_A^2n](1 + \eta) - k_2 n_A \\ &\quad + \frac{\partial}{\partial x} D_0 (1 + \gamma) \frac{\partial n_A}{\partial x} + q \left( \frac{\partial n_A}{\partial x} \right)^2. \end{aligned} \quad (45)$$

$D_0 = kT|b_0|/m$  is the diffusion coefficient for hard spheres, unperturbed by the reactions. Nonequilibrium corrections  $\eta$ ,  $\gamma$ , and  $q$  to the rate of chemical and transport processes depend on reaction parameters—activation energy and steric factors—as well as on the concentrations of the species. The elementary but lengthy expressions for these coefficients are given in the Appendix. The above modified reaction-diffusion equation is the main result of our treatment of the Boltzmann equation. The predictions for the speed and shape of the perturbed trigger front are deduced from numerical integration of Eq. (45). In Sec. V we examine these theoretical results by comparison with the microscopic simulations, in which motion of individual particles is followed. The method of the simulation is described in Sec. IV.

#### IV. MICROSCOPIC SIMULATION PROCEDURE

According to Bird's simulation method [12], the medium is divided into linearly arranged cells of length  $\Delta x$  equal to a fraction of the mean free path. Each cell is assumed to be homogeneous. During the simulation time step  $\Delta t$  chosen as a fraction of the mean free time, the free motion of particles and their mutual collisions are supposed to be uncoupled. Particle velocities are treated in three dimensions, but their positions are projected onto the direction of front propagation, and the perpendicular coordinates are disregarded. In these conditions, the sections of the cells and consequently the number density are adjustable parameters and the dilute gas assumption is not restrictive. The results presented were obtained for the following parameter values: temperature  $kT=1$ , mass  $m=1$ , diameter  $d=1$ , cell volume  $V=1$ , mean number of particles in a cell,  $N=100$ . Assigning the values of the steric factors  $s_1$  and  $s_{-1}$  and activation energy  $\epsilon$  determines the rate constants  $k_1^{(0)}$  and  $k_{-1}^{(0)}$ . Then, for a chosen value of  $b$ , the rate constant  $k_2$  follows from Eq. (8).

In order to simulate collisions, we choose randomly  $\Delta t N^2 \sigma_0 g_{max}/2$  pairs of particles in the same cell susceptible to collision in time step  $\Delta t$ . Here,  $g_{max}$  is the continuously updated maximum relative speed. The above number includes actual as well as null collisions, because it is calculated as for a hypothetical system in which the relative velocity for each pair of particles is  $g_{max}$  [30]. The standard acceptance-rejection method is then applied to choose actual encounters: The collision between a chosen pair of particles is accepted if their relative speed obeys  $g > R g_{max}$  where  $0 \leq R \leq 1$  is a random number [12]. The postcollisional relative velocity is calculated for randomly chosen impact parameter and deflection angle. In order to simulate reactions (1) of the applied version of the Schlögl model, the chemical identity of the colliding pair changes according to the proce-

dure described in the previous section. Let us give an example of the particular treatment adopted to simulate a termolecular reaction like  $(A+B)+A \rightarrow 3A$ . A collision between a particle  $A$  and a particle  $B$  is reactive (i) with the probability given by the steric factor  $s_1$ , (ii) if the condition on relative velocity given in Eq. (14) is satisfied, and (iii) if a third particle, randomly chosen in the same cell, is an  $A$ . When these three conditions are fulfilled, the particle  $B$  is transformed into  $A$ . Reaction (2) is reproduced by transforming during the time step  $\Delta t$  a number  $k_2 n_A \Delta t$  of randomly chosen  $A$  particles into  $B$  particles.

We choose as initial condition the unperturbed profile given by Eq. (9). The simulated medium is ten times longer than the front width. On the extreme left of the medium, the numbers of particles  $A$  and  $B$  in a cell initially obey  $N_A = A_1^0 V$  and  $N_B = N - N_A$ , whereas on the extreme right of the medium, one has initially  $N_A = 0$  and  $N_B = N$ .

We choose specific boundary conditions in order to mimic the propagation of a front of particles  $A$  in an infinite medium. In the case of the Fisher front [13], associated with the chemical reaction  $A+B \rightarrow 2A$ , the first (last) cell was occupied only by particles  $A(B)$ , which had an equilibrium velocity distribution [11]. It was therefore possible to couple the first and last cells by particular periodic boundary conditions, simply by changing the chemical nature of the particles that were crossing the permeable wall between the last and the first cell. For the Schlögl front, we assume that the left wall of the first cell as well as the right wall of the last cell are impermeable: particles are elastically reflected by these walls. Actually, in this case, the last cells are filled only with  $B$  particles that have an equilibrium velocity distribution since there is no reaction in the absence of  $A$  particles. However, the first cells contain both  $A$  and  $B$  particles, whose velocity distributions are perturbed due to reaction (1). In these conditions, the possible arrival of a particle  $B$  from the last cell into the first one cannot be treated properly. Moreover, in simulations we switch to the frame moving with the front: each time the total number of particles  $A$  becomes greater than its initial value, the first left cell is transformed into the last right one with simultaneous transformation of its particles  $A$  into  $B$ 's. At the same time, the front position  $\phi(t)$  is increased by  $\Delta x$ . This procedure is made possible by the fact that the mixture of particles  $A$  and  $B$  (as a whole) on the extreme left and the particles  $B$  on the extreme right both have equilibrium velocity distributions. For the parameter values chosen, this trick is actually performed only about every 100th time step on average. Note that the propagation of the front in the opposite direction, linked to a decrease of the total number of particles  $A$ , would require the suppression of the last cell containing only  $B$ 's in equilibrium and the creation of a first cell containing particles  $A$  and  $B$  with different nonequilibrium velocity distributions. It would be impossible to assign velocities to the particles of each species in the new first cell.

#### V. COMPARISON OF THE MACROSCOPIC PROPERTIES OF A TRIGGER WAVE DEDUCED FROM THE BOLTZMANN EQUATION AND FROM MICROSCOPIC SIMULATIONS

We deduce from the microscopic simulations a time average of the local fraction of particles  $A$ ,  $\langle a(\zeta) \rangle$

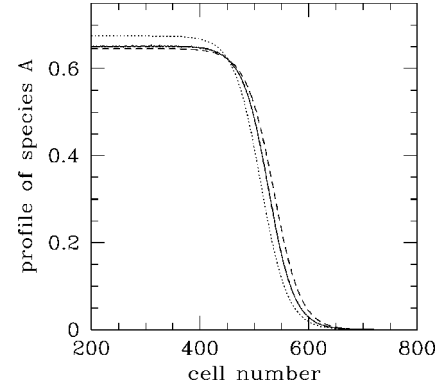


FIG. 1. Front profiles in the moving frame. The solid line corresponds to simulation results and gives the spatial variations of the time averaged fraction  $\langle a(\zeta) \rangle$  of particles  $A$ . The short-dashed line corresponds to analytical results based on the Boltzmann equation and the dotted line to the macroscopic prediction without nonequilibrium corrections. The parameters take the following values: steric factor of the forward (backward) reaction (1)  $s_1 = 1$  ( $s_{-1} = 0$ ), activation energy of reaction (1)  $\epsilon = 1$ , control parameter  $b = 0.35$ . The average is performed over a time corresponding to more than  $2.7 \times 10^8$  reactive collisions. The profiles have been slightly translated to improve readability.

$= \langle n_A(\zeta) \rangle / n$ , in cell  $\zeta$  of the moving frame. It evolves to a stationary profile and the moving frame reaches a stationary mean speed  $\langle U \rangle$ . The results given in this section are obtained for stationary conditions in the moving frame and after averaging over a time corresponding to more than  $10^8$  reactive collisions. As shown in Fig. 1, the value of the left front plateau is decreased with respect to the unperturbed stationary state value  $A_1^{(0)}/n$ , for both the profiles predicted by the theory and deduced from the simulations. The slope at the inflection point, i.e., the profile width, is not sensitively modified. It can be seen in Fig. 2 that the decrease of the front plateau is accompanied by a deviation of the kinetic energy of particles  $A$  from the equilibrium value. This increase of particle  $A$  temperature is associated with a deviation of the particle velocity distribution from the Maxwellian

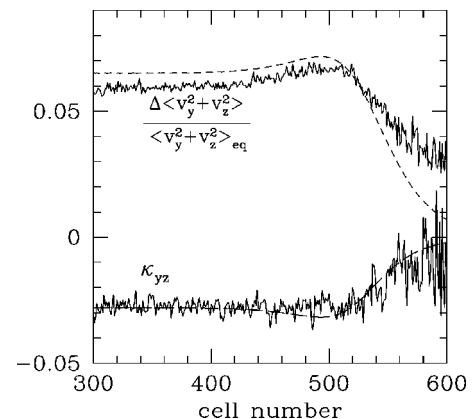


FIG. 2. Spatial variations in the moving frame of the kurtosis  $\kappa_{yz}$  of the  $A$  particle velocity distribution and of the relative deviation of its second moment  $\langle v_y^2 + v_z^2 \rangle$  from its equilibrium value. The solid lines correspond to simulation results, the dashed lines to analytical results based on the Boltzmann equation. Same parameter values as in Fig. 1.

shape, as proved by the nonvanishing values of the kurtosis. The deformation of the velocity distribution of  $A$  particles can be expressed by the moments of the distribution; we confine ourselves to the first order correction (30) determined by Eqs. (40)–(44). In order to avoid the anisotropy of velocity distribution induced by inhomogeneities in the  $x$  direction, we use the perpendicular velocity  $\mathbf{v}_\perp = (v_y, v_z)$ . The second moment  $\int f_A(\mathbf{v}, t) v_\perp^2 d\mathbf{v} = n_A(t) \langle v_\perp^2 \rangle_A$  is related to the temperature of species  $A$  by  $kT_A = \frac{1}{2} m \langle v_\perp^2 \rangle_A$ . The relative correction to  $T_A$  calculated analytically by means of the perturbation solution of the Boltzmann equation is given by

$$\frac{T_A - T}{T} = \frac{1}{2} \left( s_1 - \left( s_1 + \frac{1}{2} s_{-1} \right) \frac{n_A}{n} \right) \frac{n_A}{n} \exp(-\epsilon) \left( e_1 + \frac{1}{30} f_1 \right) \quad (46)$$

with  $e_1 = \epsilon + 1/2$  and  $f_1 = -\epsilon^2 + 2\epsilon + 3/4$ . The shape of the velocity distribution is indicated by the kurtosis  $\kappa_{yz} = (m/2kT)^2 (\langle v_\perp^4 \rangle - 2\langle v_\perp^2 \rangle^2)$  which vanishes for the Maxwellian distribution. The perturbation solution of the Boltzmann equation gives the following expression for the kurtosis:

$$\begin{aligned} \kappa_{yz} = & - \left( s_1 - \left( s_1 + \frac{1}{2} s_{-1} \right) \frac{n_A}{n} \right) \frac{n_A}{n} \exp(-\epsilon) \\ & \times \left[ \frac{2}{15} f_1 + \frac{1}{2} \left( s_1 - \left( s_1 + \frac{1}{2} s_{-1} \right) \frac{n_A}{n} \right) \frac{n_A}{n} \right. \\ & \left. \times \exp(-\epsilon) \left( e_1 + \frac{1}{30} f_1 \right)^2 \right]. \quad (47) \end{aligned}$$

As well predicted by the analytical approach, temperature shift and kurtosis reach maximum values in the steepest part of the front and tend to a nonvanishing limit in the region of the left front plateau. The deviation of macroscopic wave front properties from the values predicted in the frame of a macroscopic approach by the unperturbed equation (3) is clearly related to the frequency of reactive collisions as shown in Fig. 3: The relative deviations of left plateau height, profile width, and propagation speed from the unperturbed values given respectively by Eqs. (6), (10), and (11) decrease and eventually vanish as the activation energy  $\epsilon$  of reaction (1) increases.

The front speed appears to be the macroscopic property that is the most affected by nonequilibrium effects. According to the simulation results and for the parameter values chosen, the largest effect reaches 65% and is obtained for  $\epsilon = 1$ . As expected, the analytical predictions deduced from a perturbative approach of the Boltzmann equation are not reliable in the limit of very fast reaction. Whereas the perturbative approach predicts a positive correction to the front speed for  $\epsilon = 0$ , the simulation results lead to a negative one. Simulation results for  $\epsilon = 0$  have been tested using a larger value of the mean number of particles in each spatial cell: for  $N = 1000$  we obtain the same negative correction to front speed as for  $N = 100$ . As already mentioned at the end of Sec. II, the simulation results do not sensitively depend on  $N$  in the case of a trigger wave [18,19], contrary to the specific case of a wave front propagating into an unstable state [15,17,18]. As soon as the activation energy becomes greater

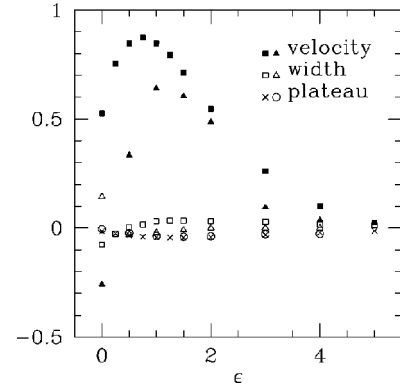


FIG. 3. Comparison between simulation results (triangles and circles) and analytical results (squares and crosses) based on the Boltzmann equation: relative deviations from their macroscopic predictions of front propagation speed (solid polygons), time-averaged profile width (open polygons), and left plateau height (crosses and circles), as functions of activation energy  $\epsilon$ . The parameters take the following values: steric factor of the forward (backward) reaction (1)  $s_1 = 1$  ( $s_{-1} = 0$ ), control parameter  $b = 0.35$ .

than 0.5, the analytical predictions based on the Boltzmann equation agree, at least qualitatively, with the simulation results. For variable  $\epsilon$ , the deviations of the second and fourth moments of the particle  $A$  velocity distribution from their equilibrium values are very well reproduced by the analytical approach based on the Boltzmann equation. As shown in Fig. 4, the analytical predictions for the limit values reached in the left front plateau by correction to particle  $A$  temperature and by kurtosis agree remarkably with the simulation results. Note that the nonvanishing corrections to macroscopic front properties, observed in Fig. 3 as  $\epsilon$  becomes smaller than 4, can be correlated with the nonvanishing corrections to equilibrium velocity distribution appearing in Fig. 4 for exactly the same range of activation energies.

We examine in Figs. 5 and 6 how the macroscopic front properties are affected by nonequilibrium effects when the control parameter  $b$ , defined by Eq. (8), varies. According to the prediction of the unperturbed macroscopic description, the front speed vanishes as  $b$  tends to  $1/3$ . This result ex-

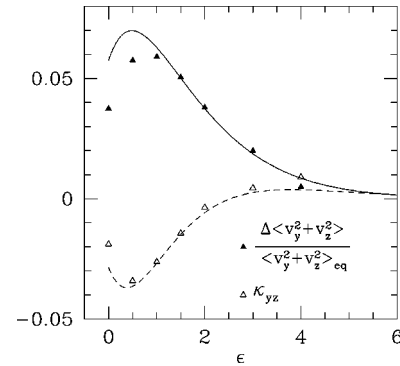


FIG. 4. Comparison between simulation results (symbols) and analytical results (lines) based on the Boltzmann equation: variations with activation energy  $\epsilon$  of the limit value reached in the left plateau of the front for the kurtosis  $\kappa_{yz}$  (open triangles and dashed line) of the  $A$  particle velocity distribution and for the relative deviation of its second moment  $\langle v_y^2 + v_z^2 \rangle$  from its equilibrium value (solid triangles and solid line). Same parameter values as in Fig. 3.

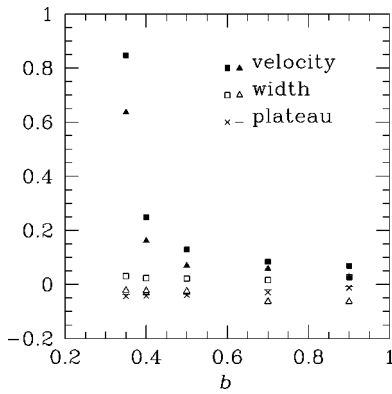


FIG. 5. Same as for Fig. 3 for a variable control parameter  $b$  and an activation energy fixed at  $\epsilon=1$ .

plains why the relative correction to front speed induced by nonequilibrium effects diverges as  $b \rightarrow 1/3$ . A different behavior is observed for the nonvanishing front properties such as width and left plateau height, whose corrections remain bounded in the vicinity of  $b=1/3$ . The growth of the distortion from the Maxwellian particle velocity distribution, observed in Fig. 6 as  $b$  decreases from 1, is related to the approach of the bifurcation predicted for  $b=0$ . Actually, we know from analysis of the Schlögl model in homogeneous conditions [7] that the bifurcation diagram is sensitively modified by nonequilibrium effects and that the bifurcation associated with the coalescence of the nonvanishing stable stationary state and the unstable one occurs earlier, for some positive value of  $b$ . We have shown that, in the vicinity of this bifurcation, the dynamical system presents an enhanced sensitivity to nonequilibrium effects. This tendency is perceivable in the case of the inhomogeneous system as  $b$  approaches  $1/3$ .

Finally, we study in Figs. 7 and 8 how the nonequilibrium corrections to macroscopic front properties vary with the steric factor  $s_{-1}$  of the backward reaction (1). As  $s_{-1}$  increases, the corrections to front properties diminish, as does the distortion to particle velocity distribution. Let us consider nonequilibrium effects induced by the reactive collisions  $(A+B)+A \rightarrow 3A$ , related to the forward reaction (1). A collision between a particle  $A$  and a particle  $B$  will be most likely accepted if  $A$  and  $B$  are both fast, so that the two  $A$ 's, which will be created in case of reaction, will also most likely be fast. It is therefore not surprising to observe an

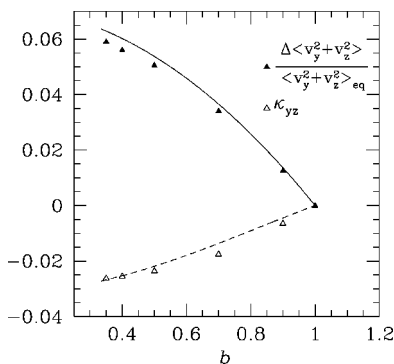


FIG. 6. Same as for Fig. 4 for a variable control parameter  $b$  and an activation energy fixed at  $\epsilon=1$ .

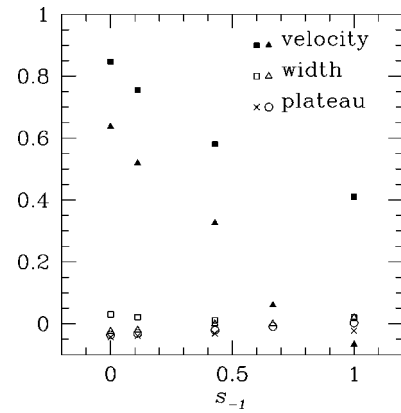


FIG. 7. Same as for Fig. 3 for a variable steric factor  $s_{-1}$  and an activation energy fixed at  $\epsilon=1$ .

increase of the kinetic energy of particles  $A$  due to forward reaction (1), and a simultaneous cooling of particles  $B$ , whose fastest representatives are transformed into  $A$ 's. Clearly, the reverse reaction (1), which creates  $B$ 's from the population of  $A$ , has the opposite tendency and weakens the effect induced by the forward reaction. As can be seen in Fig. 8, the effect of the forward reaction always prevails in the upper stationary state, because the forward process must be faster there to ensure balance between reaction (1) and irreversible reaction (2). The agreement between the theoretical predictions and simulation results worsens when  $s_{-1}$  increases. These discrepancies probably result from the exclusion correction arising in simulations due to the finite number of particles in a cell. It should be noted that the exclusion effect is much stronger for the reverse reaction (1) than for the forward reaction, because the former involves three molecules of the same species.

## VI. CONCLUSIONS

In this paper we have studied a trigger wave front propagating between the two stable stationary states of an inhomogeneous chemical system. Imposing specific conditions, we have been able to eliminate nucleation phenomena, which could disturb the front propagation. It has been proved that a departure from the equilibrium particle velocity distribution induced by a chemical reaction modifies the macroscopic properties of the front. The trigger front gives a good oppor-

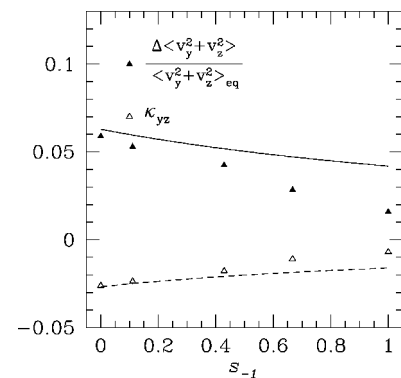


FIG. 8. Same as for Fig. 4 for a variable steric factor  $s_{-1}$  and an activation energy fixed at  $\epsilon=1$ .

tunity to study these nonequilibrium effects because in this system the perturbations due to variable discretization and internal fluctuations can be neglected. This is a great advantage over the case of a wave front propagating into an unstable state, where all the perturbations of different origins interfere [11,16].

From the perturbation solution of the Boltzmann equation we have derived a modified reaction-diffusion equation for concentrations which includes the corrections due to the nonequilibrium effects, to both the reaction and the diffusion terms. The speed and shape of the perturbed front has been calculated using a numerical solution of this modified reaction-diffusion equation. It should be emphasized that derivation of these results cannot neglect the perturbation of the diffusion process, and thus cannot be obtained from the perturbed equation for the chemical kinetics only, considered in the previous paper on the homogeneous bistable system [7]. We showed there that values of stationary states can be changed due to nonequilibrium effects. However, it can easily be calculated [from Eq. (45) with neglect of all terms related to inhomogeneities] that the relative shifts of the two stationary states  $A_1$  and  $A_2$  are approximately the same and negative. It can be seen from Eq. (11) that this will slow down propagation of the front. On the contrary, our theoretical predictions and microscopic simulations almost always give an increase of the front speed.

Provided the reaction is not very fast, the theoretical predictions based on the reaction-diffusion equation agree quite well with the results of microscopic simulations using Bird's method, even for such a sensitive quantity as the fourth order cumulant (or kurtosis) of the particle velocity distribution. Superposition of different effects prevented us from reaching such a good agreement in the previous study of a wave front propagating into an unstable state [11,16]. The nonequilibrium effects for the trigger front are strongest when the activation energy of the reaction is comparable to the thermal energy. The largest effects are observed on the speed of the front, for which the relative correction reaches 65% for parameter values close to that corresponding to a stationary interface between the two stable stationary states. The plateau height and the front width are also affected by the nonequilibrium effects, but the relative corrections in these cases do not exceed 10%. We expect stronger corrections in the vicinity of the bifurcation associated with the coalescence of the unstable stationary state with the nonvanishing stable stationary state. The previous study [7] of a homogeneous bistable system revealed the existence of diverging corrections to the nonvanishing stable stationary state value near this bifurcation. However, the conditions applied in this pa-

per allowed us on the one hand to avoid the problem of nucleation, but on the other hand prevented us from studying the vicinity of this bifurcation.

## ACKNOWLEDGMENTS

This work was possible thanks to the support of Grant No. POL/1639 from CNRS (France) and the Polish Academy of Sciences.

## APPENDIX

For the line-of-centers model of reactive hard spheres, the coefficients  $\eta$ ,  $\gamma$ , and  $q$  in Eq. (45) are given by

$$\eta = \left( s_1 - (2s_1 + s_{-1}) \frac{n_A}{n} \right) \frac{n_A}{n} \frac{1}{4} \times \exp(-\epsilon) \left[ \left( \frac{1}{2} + \epsilon \right)^2 + \frac{1}{30} \left( \frac{3}{4} + 2\epsilon - \epsilon^2 \right)^2 \right], \quad (\text{A1})$$

$$\gamma = \left( s_1 d_1 - \frac{n_A}{n} (2s_1 + s_{-1}) d_2 \right) \frac{n_A}{n}, \quad (\text{A2})$$

$$d_1 = \exp(-\epsilon) \left[ -\frac{5}{8} + 2\epsilon - \frac{1}{59} \left( \frac{5}{4} + 11\epsilon + \frac{13}{2}\epsilon^2 \right) + \left( \frac{1}{59} \right)^2 (-4 + 10\epsilon + 10\epsilon^2 + 2\epsilon^3) \right], \quad (\text{A3})$$

$$d_2 = \exp(-\epsilon) \left[ -\frac{1}{2} + \epsilon + \frac{1}{59} \left( -\frac{1}{4} + 5\epsilon - \frac{7}{2}\epsilon^2 \right) + \left( \frac{1}{59} \right)^2 \left( -3 + 4\epsilon - \frac{5}{4}\epsilon^2 \right) \right], \quad (\text{A4})$$

$$q = \frac{D_0}{n} \left( -s_1 d_3 + \frac{n_A}{n} (2s_1 + s_{-1}) d_4 \right), \quad (\text{A5})$$

$$d_3 = \exp(-\epsilon) \left[ \frac{1}{4} + \frac{1}{2}\epsilon - \frac{1}{59} \left( \frac{5}{4} + \frac{5}{3}\epsilon + \frac{5}{3}\epsilon^2 \right) - 11 \left( \frac{1}{59} \right)^2 \left( \frac{3}{4} + 2\epsilon - \epsilon^2 \right) \right], \quad (\text{A6})$$

$$d_4 = \exp(-\epsilon) \left[ \frac{5}{8} + \frac{5}{4}\epsilon - \frac{1}{59} \left( \frac{7}{2} + \frac{5}{2}\epsilon + 4\epsilon^2 \right) - \left( \frac{1}{59} \right)^2 \left( \frac{9}{2} - 5\epsilon - 5\epsilon^2 - \epsilon^3 \right) \right], \quad (\text{A7})$$

[1] I. Prigogine and E. Xhrouet, *Physica* (Amsterdam) **15**, 913 (1949); C. F. Curtiss, University of Wisconsin/Naval Research Laboratory Report No. CM-476, 1948.  
 [2] J. Ross and P. Mazur, *J. Chem. Phys.* **35**, 19 (1961).  
 [3] B. Shizgal and M. Karplus, *J. Chem. Phys.* **52**, 4262 (1970); **54**, 4345 (1971); **54**, 4357 (1971).  
 [4] See a number of papers in *Far-from-Equilibrium Dynamics of Chemical Systems*, edited by J. Gorecki *et al.* (World Scientific, Singapore, 1994).

[5] Z. Schlögl, *Z. Phys.* **253**, 147 (1972).  
 [6] R. Kapral and K. Showalter, *Chemical Waves and Patterns* (Kluwer, Dordrecht, 1995).  
 [7] A. Lemarchand and B. Nowakowski, *Physica A* **271**, 87 (1999).  
 [8] J. Boissonade, *Physica A* **113**, 607 (1982).  
 [9] F. Baras and M. Malek-Mansour, *Adv. Chem. Phys.* **100**, 393 (1997).  
 [10] M. Mareschal and A. De Wit, *J. Chem. Phys.* **96**, 2000 (1992).

- [11] A. Lemarchand and B. Nowakowski, *J. Chem. Phys.* **109**, 7028 (1998).
- [12] G. A. Bird, *Molecular Gas Dynamics and the Direct Simulation of Gas Flows* (Clarendon, Oxford, 1994).
- [13] R. A. Fisher, *Ann. Eugenics* **7**, 335 (1937).
- [14] W. van Saarloos, *Phys. Rev. Lett.* **58**, 2571 (1987).
- [15] E. Brunet and B. Derrida, *Phys. Rev. E* **56**, 2597 (1997).
- [16] A. Lemarchand and B. Nowakowski, *J. Chem. Phys.* **111**, 6190 (1999).
- [17] A. Lemarchand, A. Lesne, and M. Mareschal, *Phys. Rev. E* **51**, 4457 (1995).
- [18] M. Karzazi, A. Lemarchand, and M. Mareschal, *Phys. Rev. E* **54**, 4888 (1996).
- [19] D. A. Kessler, Z. Ner, and L. M. Sander, *Phys. Rev. E* **58**, 107 (1998).
- [20] B. Nowakowski, *J. Chem. Phys.* **109**, 3443 (1998).
- [21] S. M. Dunn and J. B. Anderson, *J. Chem. Phys.* **102**, 2812 (1995).
- [22] H. Haken, *Advanced Synergetics* (Springer, Berlin, 1983).
- [23] V. N. Kondratiev and E. E. Nikitin, *Gas-Phase Reactions* (Springer, Berlin, 1981); G. G. Hammes, *Principles of Chemical Kinetics* (Academic, New York, 1978).
- [24] E. G. D. Cohen, *Lect. Theor. Phys.* **8A**, 145 (1966); J. V. Sengers, *Phys. Fluids* **9**, 1333 (1966); J. T. Lowry and R. F. Snider, *J. Chem. Phys.* **61**, 2320 (1974).
- [25] B. Nowakowski and A. Lemarchand, *J. Chem. Phys.* **106**, 3965 (1997).
- [26] S. Chapman and T. G. Cowling, *The Mathematical Theory of Nonuniform Gases* (Cambridge University Press, Cambridge, 1970).
- [27] J. H. Ferziger and H. G. Kaper, *Mathematical Theory of Transport Processes in Gases* (North-Holland, Amsterdam, 1972).
- [28] B. Shizgal, *J. Chem. Phys.* **55**, 76 (1971); D. Napier and B. Shizgal, *Phys. Rev. E* **52**, 3797 (1995).
- [29] B. D. Shizgal and D. G. Napier, *Physica A* **223**, 50 (1996).
- [30] K. Koura, *Phys. Fluids* **29**, 3509 (1986).